"NOTICE: When Government or other drawings, specifications or other data are used for any purpose other than in connection with a definitely related Government procurement operation, the U.S. Government thereby incurs no responsibility, nor any obligation whatsoever; and the fact that the Government may have formulated furnished, or in any way supplied the said drawings, specifications or other data is not to be regarded by implication or otherwise as in any manner licensing the holder or any other person or corporation, or conveying any rights or permission to manufacture, use or sell any patented invention that may in any way be related theret

5

PURDUE UNIVERSITY

DEPARTMENT OF PHYSICS

SPECTROSCOPIC RESEARCH

TECHNICAL REPORT No. 1.

THE ARC SPECTRUM OF CESIUM

By H. Kleiman and K. W. Meissner

CONTRACT Nonr-1100(08)

BETWEEN

PURDUE RESEARCH FOUNDATION

AND

OFFICE OF NAVAL RESEARCH

OCTOBER 1959

PURDUE UNIVERSITY

DEPARTMENT OF PHYSICS

SPECTROSCOPIC RESEARCH

TECHNICAL REPORT No. 1.

THE ARC SPECTRUM OF CESIUM

By H. Kleiman and K. W. Meissner

CONTRACT Nonr-1100(08)

BETWEEN

PURDUE RESEARCH FOUNDATION

AND

OFFICE OF NAVAL RESEARCH

OCTOBER 1959

ABSTRACT*

Precision measurements ~~have been~~ were made on ~~eighty-three~~ 63 lines in the arc spectrum of ~~cesium~~ Cs. ~~In particular~~ the first ~~three~~ 3 members of the principal series ~~have been~~ were measured interferometrically for the first time, allowing improvement in the level scheme.

Comparison ~~has been~~ was made of the wavelengths emitted by ~~two~~ 2 different light sources, a Geissler tube and an Electrodeless Discharge lamp, and a relative shift ~~has been~~ was found in the high members of the fundamental series. ~~This makes it even now~~ desirable to develop an atomic beam light source which one hopes will be free of perturbations.

The term values found ~~in this investigation have been~~ were fitted to extended Ritz type formulas with fair accuracy. The polarization formula ~~has been~~ was used to fit the fundamental series.

* This work was conceived and directed by the senior author (KWM) until his death in April, 1959. The work in Section V (Analysis) of this report was completed after his death, and the junior author accepts full responsibility for the results of this section, as well as for the writing of the manuscript.

I. Introduction

Since the earliest days of atomic theory, the study of one-electron spectra has been of fundamental interest to the development of physics. It's successes have ranged from Bohr theory to the present day refinements of the Lamb Shift. The atoms of hydrogen and the alkali metals have allowed a variety of models to explain their spectra.

However, recent advances both in theoretical understanding of atomic theory and in refinement of experimental technique have made it desirable to remeasure the alkali spectra and see to what extent the older models still hold. A start in this direction has been the work at Lund under the direction of Edlén, where the spectra of the lighter alkalies, i.e., Li, Na, and K, have been remeasured. In this laboratory work has started on the heavier alkalis, i.e., K, Rb, and Cs, and the purpose of this report is to give some preliminary results on the spectrum of cesium.

II. Previous Work

The earliest work on the arc spectrum of cesium as listed in Vol. 7 of Kayser's "Handbook der Spectroscopie" is that of Paschen[1] and Randall[2]. Using concave grating and prism instruments they measured and classified about 35 lines in the infrared spectrum. Bevan[3,4] measured the first 24 members of the principal series in absorption. Using vacuum and air arcs, Meissner[5] made grating measure-

ments of many lines in the red and infrared. In 1921 the first precision measurements were carried out by Meissner[5] using a Geissler tube and a Fabry-Perot interferometer. This investigation was the first to reveal the structure of the fundamental series. Meggers[7], in 1933, carried out investigations in the infrared with a large concave grating and in particular measured the lines associated with the first member of the fundamental series. In 1937, Meissner and Weinmann[8] remeasured these lines interferometrically.

Kratz[9], in 1947, measured the principal series from n = 2 through n = 41 in absorption deriving a series limit of 31406.54 cm^{-1}. He also verified that the doublet fine structure splitting was proportional to $1/_n 3$.

Finally there are two unpublished works of Mack and Fisher whose results are quoted in C. E. Moore's Atomic Energy Levels[10]. Mack measured in absorption the forbidden transitions $n^2D_{5/2,3/2}-6^2S_{1/2}$ for n = 9 through n = 21. Fisher made some important measurements in the infrared, some of which led to the connection of the 5^2D levels with the rest of the level scheme. These levels, in turn, tie the entire fundamental series to the rest of the level scheme.

III. Experimental

A. Light Sources

The initial light source used in this investigation was an Electrodeless Discharge lamp[11]. This consists of a 4 inch length of pyrex tubing containing a few tenths of a gram of cesium metal and argon gas at a pressure of 2 mm Hg to act as a carrier. The tube was run at a frequency of 2450 Mc/sec, with power supplied by a Raytheon Microtherm microwave generator. The power was delivered by an umbrella shaped antenna (see Fig. 2a).

The system for the preparation of such tubes is shown in Fig. 1a. A reservoir containing some CsCl and an excess of calcium metal is placed in a furnace. At a temperature of 600° C the cesium is reduced to the metallic state and driven into the region of the second furnace which operates at 300° C. The cesium metal redistills and leaves behind most of the calcium which the first furnace may have driven over. The cesium is deposited in the section of pyrex tubing between the two constrictions. This section of tubing is previously outgassed at 450° C for about 8 hours to drive out any traces of mercury from the diffusion pump. After the cesium metal has been distilled into this region, the reservoir is cut off, and argon gas at a few mm Hg pressure is introduced into the system. Finally the tube itself is cut off the system at the second constriction. Others have found that running the tube for several hours while still

attached to the system helps remove traces of mercury vapor. The authors have found that careful outgassing is sufficient.

Preliminary wavelength measurements of some of the lines obtained with this source were at variance with the values obtained by Meissner in 1921. In order to determine if these discrepancies were caused by the carrier gas the lamp was modified to operate without a carrier gas. By this means any shifts introduced by collision processes with the rare gas[12] could be avoided. This modified lamp was made of quartz tubing with a few tenths of a gram of cesium metal inside. The power dissipated in operating the tube heated the cesium to a sufficiently high vapor pressure for continuous operation. (Note that in making the lamp with quartz tubing, the quartz should be outgassed at 1000° C before introducing the metal.)

This modified source was very successful. It has operated for several hundred hours and gives no indication of failing. In addition to avoiding pressure shifts, it excites several high members of the diffuse and fundamental series that the argon filled tube failed to excite. The cesium lines emitted have a considerably narrower half-width as witnessed by the fact that in several lines the $^2P_{1/2}$ hyperfine splitting (.039 cm^{-1}) was resolved with a 30 mm etalon. Consequently, the argon-filled electrodeless discharge lamp was abandoned in favor of this modified source.

A second type of source used in the present investigation was a Geissler tube built as closely identical as possible to that used by Meissner in his 1921 investigation. It had a capillary 13 cm long which was viewed end-on to increase the intensity. Further, in as much as the illumination had to cover a vertical spectrograph slit, the capillary was elliptically shaped with semi-axes of 5 mm and 1/2 mm. Helium was used as a carrier gas at a pressure of 2.5 mm Hg. The tube was filled on the system shown in Fig. 1b. In order to obtain a sufficiently high vapor pressure of cesium, the tube was operated in a furnace (Fig. 2b)

This light source excited even higher members of the various series than the Electrodeless Discharge lamp without carrier gas. However, the cesium lines emitted were not as narrow, as evidenced by the fact that the $^2P_{1/2}$ hyperfine splitting was not resolved.

B. Spectrographic Equipment

The Purdue concave grating spectrograph was used for rough, preliminary, wavelength measurements. This grating has a 30 foot radius of curvature and a theoretical resolving power in the first order of 80,000. Its reciprocal dispersion in this order is approximately 1.8 A/mm.

The external optics used with the grating are shown in Fig. 3a. The cesium source was focused on the grating slit by means of a concave mirror. The standard source,

which in this case consisted of either a Pfund arc or a neon Geissler tube, produced a virtual image at Sirks focus[13]. This produced a reduced image at the camera allowing an easy separation of standard and source.

The optical arrangement used in making the precision measurements is shown in Fig. 3b. This consists of a Fabry-Perot interferometer crossed with a prism spectrograph. The prism instrument, which was developed with funds from the earlier Navy contract (N7onr-39421), has a reciprocal dispersion which varies from 50 A/mm at 5200 A to 240 A/mm at 9100 A. It was adjusted for minimum deviation of the mercury green line.

The Fabry-Perot was used in external mounting. The interferometer plates were of crystalline quartz, 65 mm in diameter, cut perpendicular to the optic axis. The spacers were of invar and polished to give parallelism to within 1/10 of a wavelength of yellow light. The entire interferometer was housed in a temperature-controlled, pressure-tight chamber which was filled with dry air at atmospheric pressure. The illumination lens was a 19 cm glass achromat and the lens which projected the fringe system on the slit was a 40 cm glass achromat. Light from the standard source, a mercury 198 water-cooled Meggers lamp, was simultaneously passed through the interferometer by reflection from a plane glass plate. The time of exposure for the cesium sources was usually quite a bit longer than that of the Meggers tube. To keep the conditions of exposure of the two sources as nearly identical as possible,

the exposure of the Meggers tube was broken into a number of equal intervals spaced uniformly throughout the exposure of the cesium source.

C. Reduction of Measurements

The grating plates were measured on a Zeiss Abbe Comparator which could be set on well defined lines with an accuracy of ± .001 mm. The wavelengths were determined by linear interpolation corrected by a curve drawn from several standard lines[14]. The estimated accuracy is ± .05 A which is sufficient to determine the correct integral order number for the shortest etalon spacer used.

Interferograms were taken, whenever possible, with both the Geissler tube and the electrodeless discharge tube. Spacers of 8, 18 and 30 mm were used. Thus a sufficient number of measurements were obtained to determine the dispersion of phase change at the interferometer surfaces and to check the consistency of the measurements. For each combination of source and spacer a line was measured on at least two different exposures, and on more than two when circumstances such as wide fringes or gross disagreement between the two measured values warranted it. Four to six fringes were each measured three times and the average values were used in the reduction of the data. The method of reduction was that used by Meissner[15]. The fractional order number was obtained to an estimated accuracy of ± .003 reflecting a wavelength accuracy which varies from ± .001 A

at 5,000 A to ± .002 A at 10,000 A, using a 30 mm etalon.

All interferometer measurements were made relative to the green line of mercury, λ 5460.7532 A, as emitted by a water-cooled Meggers lamp originally filled with argon at a pressure of 3 mm Hg. This value was decided upon by using the recently provisionally adopted[16] vacuum value of λ 5462.2707 A, correcting this value to standard air with the Edlen Tables[17] and adding a pressure shift[18] of .0001 A* due to the presence of argon gas. The wavelengths were corrected to standard conditions and corrections for the dispersion of air[19] were applied using the Edlén Tables. Finally dispersion of phase change corrections[15] were made from the graph in Fig. 4.

IV. Results

The results of the measurements are conveniently displayed in a series of tables. Table I gives a complete list of wavelengths measured, the light source used, and the longest spacer used, so that a realistic estimate of the accuracy may be made. As a check upon the accuracy of the measurements, one can apply the Ritz Combination Principal. Below is a list of the splitting of the 6^2P

* The pressure shift due to the argon gas was found by Baird to be .00006 A/mm Hg. As the Meggers tube used was an old one, it was assumed that the pressure of argon gas had dropped to about 1.5 mm Hg by the "cleanup" process.

fine structure as measured in the Sharp and Diffuse series. Except for the $10^2S_{1/2}$ transitions this is consistent with an error in individual level measurements of .001 cm^{-1}.

Sharp Series		Diffuse Series	
$(nS_{1/2}-6P_{1/2}) - (nS_{1/2}-6P_{3/2})$		$(nD_{3/2}-6P_{1/2}) - (nD_{3/2}-6P_{3/2})$	
n	$^2P_{1/2,3/2}$ (cm^{-1})	n	$P_{1/2,3/2}$ (cm^{-1})
8	554.039	6	554.038
9	554.036	7	554.038
10	554.051	8	554.040
11	554.039	11	554.037
12	554.036		

If one uses the splittings of the ^2F state as measured by Meissner, one can then use differences of terms in the fundamental series to obtain the splitting of the 5^2D state, as shown below:

$$(n^2F_{5/2} - 5^2D_{3/2}) - (n\ ^2F_{7/2,5/2})$$

n	$5^2D_{5/2,3/2}$ (cm^{-1})
4	97.588
5	97.587
6	97.591
7	97.591

Again this is consistent with errors of .001 cm^{-1}.

In Table II the wavelengths as emitted by the two different light sources are compared. It is to be noted that the agreement is within experimental error except for the higher members of the fundamental series (See Fig. 5). It is tempting to ascribe these differences to collision processes since the F terms belong to non-penetrating orbits and thus should lend themselves to interatomic Stark perturbations. Further, the shift is in the correct direction to be attributed to He-Cs collisions.* However, the exact nature of the shifts is not clearly understood at present, and more work must be done in this direction.

From the wave numbers in Table I a level scheme has been derived. This is displayed in Fig. 6 and Table III. In this scheme Fisher's values for the 5^2D terms have been adopted. As the accuracy of his measurements is unknown, this term and all of the ^2F terms which are based on this term are subject to a constant uncertainty, X.

In Fig. 7 the doublet fine structure splitting of the ^2D and ^2F terms are plotted as a function of the effective quantum number n^* and found to vary roughly as $1/n^{*3}$. The discrepencies in the high members of the ^2D terms, which Condon and Shortly[20] mention, do not seem to be present.

* (See Fig. 9 of Ref. 12)

TABLE I

WAVELENGTHS MEASURED IN CESIUM I.

λ air (A)	$\tilde{\nu}$ vac. (cm^{-1})	Transition	Source	Spacer
10123.6000	9875.202	$4^2F_{7/2} - 5^2D_{5/2}$	Geissler	30 mm
10024.3594	9972.966	$4^2F_{5/2} - 5^2D_{3/2}$	Geissler	30 mm
9208.5359	10856.510	$6^2D_{3/2} - 6^2P_{3/2}$	Geissler	30 mm
9172.3216	10899.374	$6^2D_{5/2} - 6^2P_{3/2}$	Geissler	30 mm
8943.4600	11178.286	$6^2P_{1/2} - 6^2S_{1/2}$	Electrodeless Discharge	8 mm
8761.4151	11410.548	$6^2D_{3/2} - 6^2P_{1/2}$	Geissler	30 mm
8521.1220	11732.320	$6^2P_{3/2} - 6^2S_{1/2}$	Electrodeless Discharge	30 mm
8079.0348	12374.318	$5^2F_{7/2} - 5^2D_{5/2}$	Geissler	30 mm
8015.7247	12472.052	$5^2F_{5/2} - 5^2D_{3/2}$	Geissler	30 mm
7943.8837	12584.840	$8^2S_{1/2} - 6^2P_{3/2}$	Geissler	30 mm
7808.9037	13138.881	$8^2S_{1/2} - 6^2P_{1/2}$	Geissler	30 mm
7279.9553	13732.564	$6^2F_{7/2} - 5^2D_{5/2}$	Geissler	30 mm
7228.5314	13830.257	$6^2F_{5/2} - 5^2D_{3/2}$	Geissler	30 mm
6983.4906	14315.538	$7^2D_{3/2} - 6^2P_{3/2}$	Geissler	30 mm
6973.2959	14336.467	$7^2D_{5/2} - 6^2P_{3/2}$	Geissler	30 mm
6870.4527	14551.067	$7^2F_{7/2} - 5^2D_{5/2}$	Geissler	30 mm
6824.6483	14648.727	$7^2F_{5/2} - 5^2D_{3/2}$	Geissler	30 mm
6723.2853	14869.576	$7^2D_{3/2} - 6^2P_{1/2}$	Geissler	30 mm
6628.6559	15081.850	$8^2F_{7/2} - 5^2D_{5/2}$	Geissler	30 mm
6586.5072	15178.362	$9^2S_{1/2} - 6^2P_{3/2}$	Geissler	30 mm
6586.019 *	15179.489	$8^2F_{5/2} - 5^2D_{3/2}$		

* Measured by Meissner. See Ref. 6.

λ air (Å)	$\tilde{\nu}$ vac. (cm^{-1})	Transition	Source	Spacer
6472.6155	15445.437	$9^2F_{7/2} - 5^2D_{5/2}$	Geissler	30 mm
6431.9629	15543.057	$9^2F_{5/2} - 5^2D_{3/2}$	Geissler	30 mm
6365.5172	15705.303	$10^2F_{7/2} - 5^2D_{5/2}$	Geissler	30 mm
6354.5531	15732.398	$9^2S_{1/2} - 6^2P_{1/2}$	Geissler	30 mm
6326.1983	15802.912	$10^2F_{5/2} - 5^2D_{3/2}$	Geissler	30 mm
6288.5866	15897.428	$11^2F_{7/2} - 5^2D_{5/2}$	Geissler	30 mm
6250.2114	15995.034	$11^2F_{5/2} - 5^2D_{3/2}$	Geissler	30 mm
6231.31	16043.6	$12^2F_{7/2} - 5^2D_{5/2}$	Geissler	Grating
6217.5986	16078.932	$8^2D_{3/2} - 6^2P_{3/2}$	Electrodeless Discharge	8 mm
6213.0993	16090.575	$8^2D_{5/2} - 6^2P_{3/2}$	Geissler	30 mm
6193.68	16141.0	$12^2F_{5/2} - 5^2D_{3/2}$	Geissler	Grating
6187.56	16157.0	$13^2F_{7/2} - 5^2D_{5/2}$	Geissler	Grating
6153.23	16247.1	$14^2F_{7/2} - 5^2D_{5/2}$	Geissler	Grating
6150.34	16254.9	$13^2F_{5/2} - 5^2D_{3/2}$	Geissler	Grating
6116.50	16344.7	$14^2F_{5/2} - 5^2D_{3/2}$	Geissler	Grating
6034.0870	16567.928	$10^2S_{1/2} - 6^2P_{3/2}$	Geissler	30 mm
6010.4900	16632.972	$8^2D_{3/2} - 6^2P_{1/2}$	Geissler	30 mm
5845.1360	17103.501	$9^2D_{5/2} - 6^2P_{3/2}$	Geissler	30 mm
5838.8276	17121.979	$10^2S_{1/2} - 6^2P_{1/2}$	Geissler	30 mm
5745.7209	17399.430	$11^2S_{1/2} - 6^2P_{3/2}$	Geissler	30 mm
5664.0165	17650.417	$9^2D_{3/2} - 6^2P_{1/2}$	Geissler	30 mm
5636.67	17736.1	$10^2D_{3/2} - 6^2P_{3/2}$	Geissler	Grating
5635.2097	17740.644	$10^2D_{5/2} - 6^2P_{3/2}$	Geissler	30 mm
5573.6740	17936.506	$12^2S_{1/2} - 6^2P_{3/2}$	Geissler	30 mm
5568.4078	17953.469	$11^2S_{1/2} - 6^2P_{1/2}$	Geissler	30 mm
5503.8524	18164.046	$11^2D_{3/2} - 6^2P_{3/2}$	Geissler	18 mm
5502.8810	18167.253	$11^2D_{5/2} - 6^2P_{3/2}$	Geissler	30 mm

λ air (Å)	ν vac. (cm^{-1})	Transition	Source	Spacer
5465.9414	18290.028	$10^2D_{3/2} - 6^2P_{1/2}$	Geissler	30 mm
5461.9231	18303.484	$13^2S_{1/2} - 6^2P_{3/2}$	Geissler	30 mm
5414.28	18464.5	$12^2D_{3/2} - 6^2P_{3/2}$	Geissler	Grating
5413.6145	18466.813	$12^2D_{5/2} - 6^2P_{3/2}$	Geissler	30 mm
5406.6672	18490.542	$12^2S_{1/2} - 6^2P_{1/2}$	Geissler	30 mm
5350.3512	18685.165	$13^2D_{5/2} - 6^2P_{1/2}$	Geissler	30 mm
5303.7766	18849.245	$14^2D_{5/2} - 6^2P_{3/2}$	Geissler	30 mm
5301.40	18857.7	$13^2S_{1/2} - 6^2P_{1/2}$	Geissler	Grating
5256.5633	19018.543	$12^2D_{3/2} - 6^2P_{1/2}$	Geissler	Grating
5196.7343	19237.497	$13^2D_{3/2} - 6^2P_{1/2}$	Geissler	Grating
5152.6813	19401.967	$14^2D_{3/2} - 6^2P_{1/2}$	Geissler	Grating
4593.1688	21765.364	$7^2P_{1/2} - 6^2S_{1/2}$	Electrodeless Discharge	8 mm
4555.2765	21946.414	$7^2P_{3/2} - 6^2S_{1/2}$	Electrodeless Discharge	8 mm
3888.6075	25708.861	$8^2P_{1/2} - 6^2S_{1/2}$	Electrodeless Discharge	8 mm
3876.1428	25791.534	$8^2P_{3/2} - 6^2S_{1/2}$	Electrodeless Discharge	8 mm

TABLE II

GEISSLER TUBE vs. ELECTRODELESS DISCHARGE LAMP

Geissler Tube (A)	Electrodeless Discharge (A)	Geissler - ED (A)
10123.6000	10123.5992	+ .0008 *
10024.3594	10024.3568	+ .0026 *
9208.5359	9208.5357	+ .0002
9172.3216	9172.3202	+ .0014
8761.4151	8761.4115	+ .0036
8079.0348	8079.0335	+ .0013 *
8015.7247	8015.7251	- .0004
7943.8837	7943.8833	+ .0004
7608.9037	7608.9050	- .0013
7279.9553	7279.9560	- .0007 *
7228.5314	7228.5333	- .0019 *
6870.4527	6870.4553	- .0027 *
6824.6483	6824.6520	- .0037 *
6723.2853	6723.2839	+ .0014
6628.6559	6628.6601	- .0042 *
6586.5072	6586.5102	- .0030
6472.6155	6472.6226	- .0071 *
6431.9629	6431.9693	- .0064 *
6354.5531	6354.5533	- .0002
6213.1005	6213.0993	+ .0012
6034.0891	6034.0870	+ .0021

Geissler Tube (A)	Electrodeless Discharge OAP	Geissler - ED (A)
6010.4893	6010.4900	- .0007
5664.0165	5664.0177	- .0012
5635.2097	5635.2128	- .0031
5502.8810	5502.8840	- .0030
5465.9414	5465.9434	- .0020

* Fundamental Series

TABLE III

LEVEL SCHEME OF CESIUM I

LEVEL		J	(cm^{-1})	Interval
6s ^2S		1/2	0.000	
6p ^2P		1/2	11178.282	554.038
		3/2	11732.320	
5d ^2D	*	3/2	14499.490	97.589
	*	5/2	14597.08	
7s ^2S	*	1/2	18535.51	
7p ^2P		1/2	21765.364	181.050
		3/2	21946.414	
6d ^2D		3/2	22588.830	42.865
		5/2	22631.695	
8s ^2S		1/2	24317.161	
4f ^2F		7/2	24472.282	.174
		5/2	24472.456	
8p ^2P		1/2	25708.861	82.673
		3/2	25791.534	
7d ^2D		3/2	26047.858	20.930
		5/2	26068.788	
9s ^2S		1/2	26910.683	
5f ^2F		7/2	26971.398	.144
		5/2	26971.542	
8d ^2D		3/2	27811.254	11.641
		5/2	27822.895	
10s ^2S		1/2	28300.249	
6f ^2F		7/2	28329.644	.103
		5/2	28329.747	

* From Fisher's Measurements

LS	LEVEL	J	(cm^{-1})	Interval
9d	9d ^2D	3/2	28828.699	7.123
		5/2	28835.822	
11s	11s ^2S	1/2	29131.751	
7f	7f ^2F	7/2	29148.147	.070
		5/2	29148.217	
10d	10d ^2D	3/2	29468.310	4.655
		5/2	29472.965	
12s	12s ^2S	1/2	29668.827	
8f	8f ^2F	7/2	29678.930	.049
		5/2	29678.979	
11d	11d ^2D	3/2	29896.365	3.209
		5/2	29899.574	
13s	13s ^2S	1/2	30035.805	
9f	9f ^2F	7/2	30042.517	.030
		5/2	30042.547	
12d	12d ^2D	3/2	30196.825	2.309
		5/2	30199.134	
10f	10f ^2F	7/2	30302.383	.019
		5/2	30302.402	
13d	13d ^2D	3/2	30415.779	1.707
		5/2	30417.486	
11f	11f ^2F	7/2	30494.508	.016
		5/2	30494.524	
14d	14d ^2D	3/2	30508.249	1.317
		5/2	30581.566	
12f	12f ^2F		30640.6	
13f	13f ^2F		30754.1	
14f	14f ^2F		30844.2	

V. Analysis

A. Series Limits

If one assumes that a given series of terms, T_n, obeys perfectly a Ritz type formula, $T_n = R\,(n + a + bT_n)^2$, then 3 levels, L_n, L_{n+1}, L_{n+2}, suffice to determine the series limit L, ($L = L_n + T_n$) and the two parameters a, b of the Ritz formula. As we go to higher n values along a series we expect a closer fit to a Ritz formula. Consequently, if we take the levels in groups of three, L_n, L_{n+1}, L_{n+2}, we should get a curve which asymptotically approaches the correct series limit. Fig. 8 shows the curves obtained for the $^2S_{1/2}$ and the $^2D_{3/2}$ levels. The $^2D_{3/2}$ curve gives an asymptotic value for the series limit of 31406.490 $\pm$ .02 cm^{-1} in good agreement with that of Kratz determined as 31406.54 $\pm$ .03 cm^{-1}.

In a similar way for the fundamental line series we get the values of 16809.570 cm^{-1} for $5^2D_{5/2} - n^2F_{7/2}$ and 16907.187 cm^{-1} for $5^2D_{3/2} - n^2F_{5/2}$. If we use Fisher's value for the 5^2D terms, we obtain a series limit of 31406.677 $\pm$ (X + .02). Note that the difference, 97.617 $\pm$ .04 cm^{-1}, between the two limits of the fundamental line series which should equal the splitting of the 5^2D state agrees within the limits of error with our measured value of 97.589 $\pm$ .001 cm^{-1}.

In Fig. 9 we give a plot of the variation with n of the quantum defect. The difference between the quantum defect of each term and that of the lowest term of the series to which it belongs is plotted against the difference

between the term value and term value of the lowest term. Notice the almost linear behavior of the ^2D terms for high quantum numbers.

B. The Extended Ritz Term Formula

The quantum mechanical justification of the Ritz formula $T_n = R(n + a + b\,T_n)$ or its equivalent form $\Delta_n = (n^*-n) = a + b\,T_n$, and the natural extension of this formula to an expansion of Δ, the quantum defect, as a power series in T_n was first given in a series of papers by Hartree[21]. Jastrow[22] discussed the problem of the two parameter Ritz formula quantum mechanically. This work found practical application in the work of Edlén and Risberg[23] on the Ca II spectrum.

In applying the theory, Edlén and Risberg use the necessary number of lower lying terms to calculate the constants in a two, three, or four parameter expansion of the quantum defect, and then calculate the higher terms with this formula. They give explicit algebraic expressions for the parameters as functions of the term values in their paper, and these expressions are used in the present work. The calculated values of the higher terms agree with the observed values to within $\pm$ .02 cm^{-1}, twenty times the uncertainty in the experimental level values. For the $^2P_{1/2,3/2}$ terms only three terms were measured, allowing a three parameter fit, but no check on the accuracy of

the formula.

The formulas obtained are tabulated below:

TABLE IV

Series	Formula for Quantum Defect
$^2S_{1/2}$	$= -4.049362 - 2.166419 \times 10^{-6} T_n - 1.978888 \times 10^{-11} T_n^2 + 1.990689 \times 10^{-16} T_n^3$
$^2P_{1/2}$	$= -3.591514 - 3.313174 \times 10^{-6} T_n - 3.010017 \times 10^{-11} T_n^2$
$^2P_{3/2}$	$= -3.559001 - 3.419142 \times 10^{-6} T_n - 3.103558 \times 10^{-11} T_n^2$
$^2D_{3/2}$	$= -2.475455 - .068460 \times 10^{-6} T_n + .025395 \times 10^{-11} T_n^2 + .269807 \times 10^{-16} T_n^3$
$^2D_{5/2}$	$= -2.466200 - .181627 \times 10^{-6} T_n + .037355 \times 10^{-11} T_n^2 + .190877 \times 10^{-16} T_n^3$
$^2F_{5/2}$	$= -0.033077 + 1.639664 \times 10^{-6} T_n$
$^2F_{7/2}$	$= -0.033171 + 1.646241 \times 10^{-6} T_n$

To show how increasing the number of parameters increases the accuracy of the fit, Tables V - VII are given below. Parenthesis about a term indicates that it was used in deriving the parameters. Column heading I implies a two parameter fit of the type $\Delta_n = a + b\,T_n$, column heading II is a three parameter fit, $\Delta_n = a + b\,T_n + c\,T_n^2$, column heading III is a modified three parameter fit $\Delta_n = a + b\,T_n + d\,T_n^3$ and column heading IV is a four parameter fit $\Delta = a + b\,T_n + c\,T_n^2 + d\,T_n^3$.

TABLE V

$^2S_{1/2}$: $T_{calc} - T_{obs}$ (A)

n	I	II	III	IV
6	- 245.516	(+ .001)	(+ .005)	+ (.005)
7 *	- 6.23	-1.44	- 3.50	+ .14
8	- (.001)	(.000)	(.000)	+ (.000)
9	- (.001)	(.000)	(+ .001)	+ (.003)
10	- .098	- .033	- .076	+ (.000)
11	- .120	- .041	- .094	+ .000
12	- .109	- .036	- .084	+ .002
13	- .100	- .038	- .082	+ .005

TABLE VI

$^2D_{3/2}$: $T_{calc} - T_{obs}$ (A)

n	I	II	III	IV
6	(.006)	(- .003)	(+ .001)	(+ .001)
7	(.002)	(- .003)	(- .003)	(- .001)
8	.880	(- .002)	(- .001)	(.000)
9	.968	- .039	+ .018	(.000)
10	.839	- .051	+ .032	+ .003
11	.689	- .050	+ .037	+ .007
12	.548	- .040	+ .039	+ .011
13	.436	- .036	+ .033	+ .008
14	.348	- .033	+ .026	+ .006

* This term was determined by Fisher and its accuracy is unknown.

TABLE VII

^2F: $T_{calc} - T_{obs}$ (A)

n	I	II
4	- .60	- .326
5	(.000)	(.000)
6	(.000)	(- .001)
7	- .010	(.000)
8	- .008	+ .005
9	+ .002	+ .015
10	+ .015	+ .027
11	+ .019	+ .027

C. Polarisation Formula

Bohr[24] was the first to point out that the polarisation of the atom core in the field of the valence electron will produce a quantum defect for non-penetrating orbits in alkali-like spectra. Born and Heisenberg[25] treated this effect on the basis of the old quantum theory and Waller[26] gave the quantum mechanical theory. In 1933 Mayer and Mayer[27] considered terms corresponding to orbits which are no longer strictly non-penetrating. They applied two additional corrections, one for the quadrupole distortion of the ion core and one for the penetration effect. Sternheimer[28] also discusses the quadrupole polarisability.

Bockasten[29] writes the equation for the term value as: $T_n = \frac{R}{n^2} + A\,\phi(n,l) + B\,\chi(n,l)$.

Here A and B are connected with the dipole polarizability, α_d, of the ion core, and the quadrupole polarizability, α_q, of the ion core, by the relations $A = R\alpha_d Z_o^4/a_o^3$ and $B = R\alpha_q Z_o^6/a_o^5$ with R the Rydberg constant, Z_o the net charge of the ion core and a_o the Bohr radius. $\Phi(n,l)$ and $\Psi(n,l)$, which contain all the (n,l) dependence of the term defect $(T_n - R_{o/n}2)$ are respectively equal to $a_o^4\langle r^{-4}\rangle/Z_o^4$ and $a_o^6\langle r^{-6}\rangle/Z_o^6$. Here r is the radius vector from the nucleus to the valence electron, and $\langle r^{-n}\rangle$ is the quantum mechanical average of r^{-n}. Bockasten gives tables of numerical values of Φ and Ψ.

Using the above formulas Bockasten found that all the observed nf ^2F terms of Mg II could be fit within the experimental uncertainties of .02 cm^{-1}, if the parameters A and B were determined from the experimental values of the 4f and 5f levels. These same parameters fit the ^2H and ^2G series with only slight deviations. Further when the formula was fit to the nd^2D series of Li I, it represented the precision measurements of Meissner, Mundie and Stelson[30] to within an accuracy of .002 cm^{-1}.

In the spectrum of Cs I a fit of the nf$^2F_{7/2}$ series to the above formula was tried, determining the parameters with the 4f and 5f terms. The results are shown in Table VIII, column I. The deviations of .02 cm^{-1} from observed term values is much larger than the experimental error. To see if these deviations were caused by higher multipole distortions of the core, the formula for the term defect

was modified to:

$$T_n - \frac{R}{n^2} = A\,\Phi(n,l) + B\,\Psi(n,l) + C\,\varphi(n,l)$$

with C proportional to the octupole polarisability and $\varphi(n,l) = a_o^8\langle r^{-8}\rangle/Z_o^8$. The method of Van Vleck[31] was used to calculate $\langle r^{-8}\rangle$ and the results for l = 3 are given in Table IX.

The result of this three parameter fit to the series is shown in column II of Table VIII. There is no improvement. Thus one is led to believe that the penetration effect, rather than the presence of higher moments, limits the accuracy of the formula in this case. This seems reasonable, in as much as Mayer and Mayer calculate penetration energies for the 4f, 5f, and 6f terms of 2.73 cm^{-1}, 2.26 cm^{-1}, and 1.58 cm^{-1} respectively, which are not negligible. It would be of great interest to calculate the penetration energy for the higher terms, subtract it to obtain a "reduced" term value and see how well the reduced term values can be fit.

TABLE VIII

	$T_{obs} - T_{calc}$ (A)	
n	I	II
4	(.000)	(.000)
5	(.000)	(.000)
6	+ .038	(.000)
7	+ .032	- .014
8	+ .017	- .027
9	+ .001	- .035
10	- .016	- .046
11	- .022	- .047

I: $\Delta L = 1.65252 \times 10^6 \Phi(n,1) + 1.84993 \times 10^7 \chi(n,1)$

II: $\Delta L = 1.32198 \times 10^6 \Phi(n,1) + 2.66553 \times 10^7 \chi(n,1) + 1.3684 \times 10^7 \theta(n,1)$

TABLE IX

n	$\sigma(n,3) \times 10^{10}$
4	4,367
5	1,762
6	885
7	509
8	322
9	216
10	152
11	112

Bibliography

1. F. Paschen "Zur Kenntnis Ultraroter Linienspektra", Ann. d. Phys. (4) 33, 717 (1910).
2. H. M. Randall "Zur Kenntnis Ultraroter Linienspektra", Ann. d. Phys. (4) 33, 739 (1910).
3. P. V. Bevan "The Absorption Spectra of Lithium and Cesium", Proc. Roy. Soc. A. 85, 54 (1911).
4. P. V. Bevan "Spectroscopic Observations: Lithium and Cesium", Proc. Roy. Soc. A. 86, 320 (1912).
5. K. W. Meissner "Untersuchungen und Wellenlangenmessungen im Rote and Infraroten Spectralbesirk", Ann. d. Phys. (4) 50, 713 (1916).
6. K. W. Meissner "Die Bergmannserie von Caesium", Ann. d. Phys. (4) 65, 378 (1921).
7. W. Meggers "Long Wavelength Arc Spectra of the Alkalis", J. Res. Bur. Standards 10, 669 (1933).
8. Meissner and Weinmann "Zur Kenntnis der Bergmannserie des Cesiums", Ann. d. Phys. (5) 29, 758 (1937).
9. Krats "Principal Series of Potassium, Rubidium and Cesium", Phys. Rev. 75, 1844 (1949).
10. C. E. Moore Atomic Energy Levels Vol. III., N.B.S. Circular 467, 124 (1958).
11. Corliss, Bozman and Westfall "Metal Halide Lamps" J. Opt. Soc. Am. 43, 398 (1953).
12. Ch'en and Takeo "Broadening and Shift of Spectral Lines Due to the Presence of Foreign Gases", Rev. Mod. Phys. 29, 20 (1957).
13. R. Sawyer Experimental Spectroscopy, Page 136 Prentiss-Hall 1951.

14. ibid. Page 246.

15. K. W. Meissner "Interference Spectroscopy", Part I, J. Opt. Soc. Am. 31, 405 (1941)

16. K. M. Baird "On the Accuracy of Wavelength Comparison", Symposium on Interferometry, National Physical Labs., Teddington. (1959).

17. B. Edlén "Vacuum Correction for Wavelengths from 2,000 to 13,500 A" Lund, Sweden (1952).

18. K. M. Baird and D. S. Smith "Measurement by Photoelectric Fringe Scanning of the Pressure Shift of Hg-198 Emission Lines" Canadian Journal of Physics 35, 455 (1957).

19. B. Edlén "The Dispersion of Standard Air", J. Opt. Soc. Am. 43, 339 (1953).

20. Condon and Shortley The Theory of Atomic Spectra, Page 145 Cambridge Press (1953).

21. D. Hartree "The Wavemechanics of an Atom with a Non-coulombic Central Field" Proc. Camb. Phil. Soc. 24, 89, 111, 426 (1924).

22. R. Jastrow "On the Rydberg-Ritz Formula in Quantum Mechanics" Phys. Rev. 73, 60 (1948).

23. Edlén and Risberg "The Spectrum of Singly-ionised Calcium" Arkiv f. Fysik 10, 553 (1956).

24. N. Bohr "Linienspektren und Atombau" Ann. d. Phys. (4) 71, 228 (1923).

25. Born and Heisenberg "Über den Einfluss der Deformierbarke der Ionen auf Optische und Chemische Konstanten" Zeits. f. Phys. 23, 388 (1924).

26. I. Waller "Die Rydbergkorrektion die Spectra von He und Li+" Zeits. f. Phys. 38, 635 (1926).

27. Mayer and Mayer "The Polarisability of Ions from Spectra" Phys. Rev. 43, 605 (1933).

28. R. M. Sternheimer "Electronic Polarisabilities of Ions from the Hartree-Fock Wave Functions" Phys. Rev. 96, 951 (1954).

29. K. Bockasten "A Study of C IV" Arkiv f. Fysik 10, 567 (1956).

30. Meissner, Mundie and Stelson "Structure of the ^2D Terms in the Arc Spectrum of Li." Phys. Rev. 74, 932 (1948); Phys. Rev. 75, 891 (1949).

31. J. H. Van Vleck "A New Method of Calculating the Mean Value of $1/r^8$ for Keplerian Systems in Quantum Mechanics" Proc. Roy. Soc. London A 143, 679 (1934).

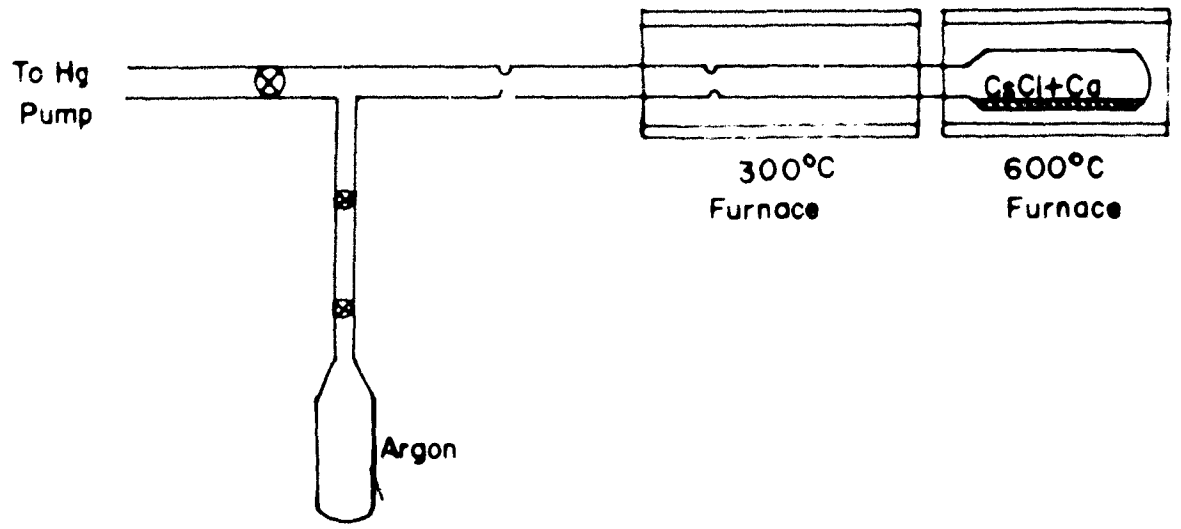

Fig Ia System For Making Electrodeless Discharge Lamps

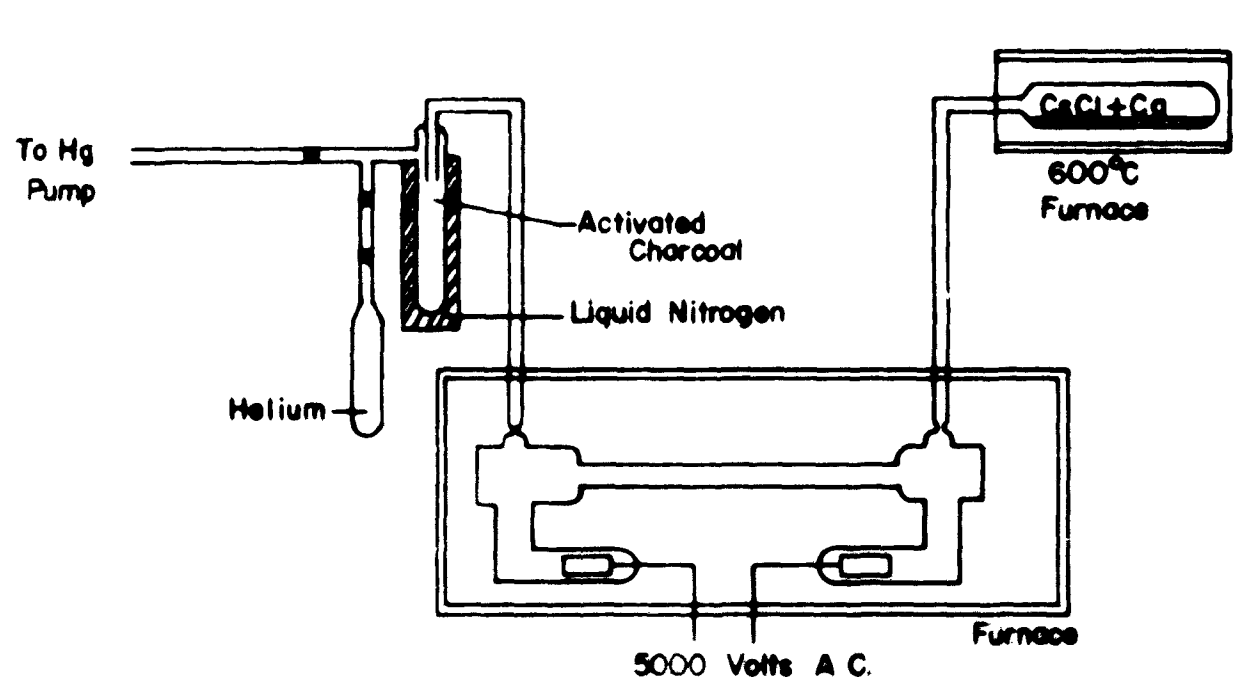

Fig Ib System For Filling Geissler Tube

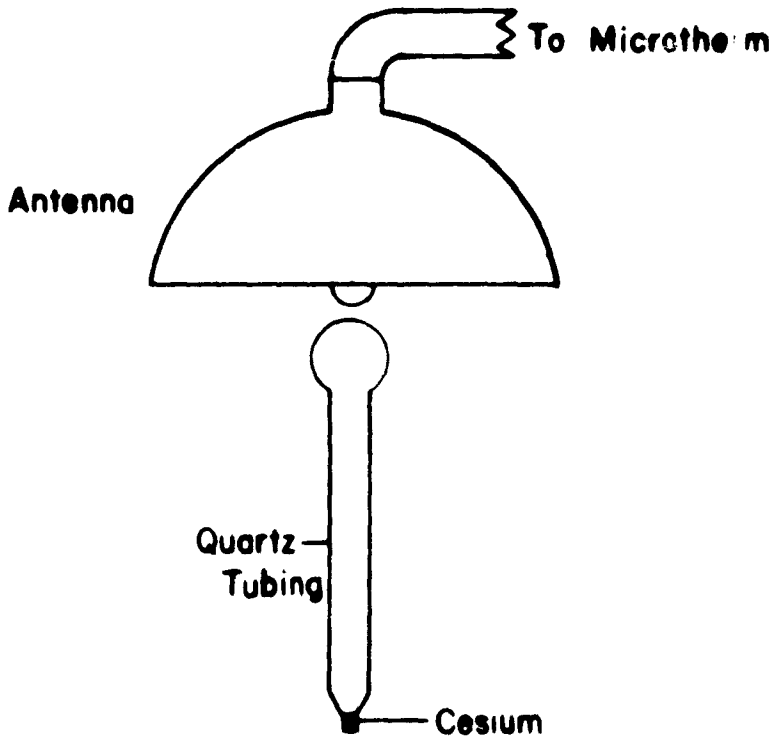

Fig 2a Electrodeless Discharge Tube

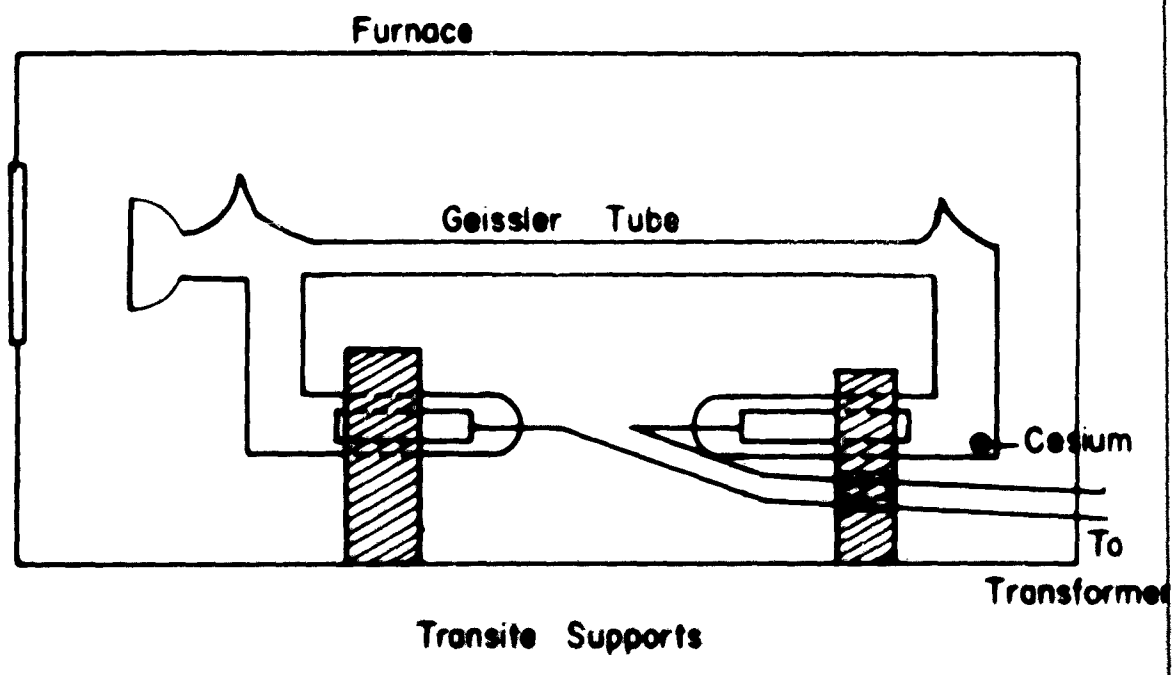

Fig 2b Geissler Tube

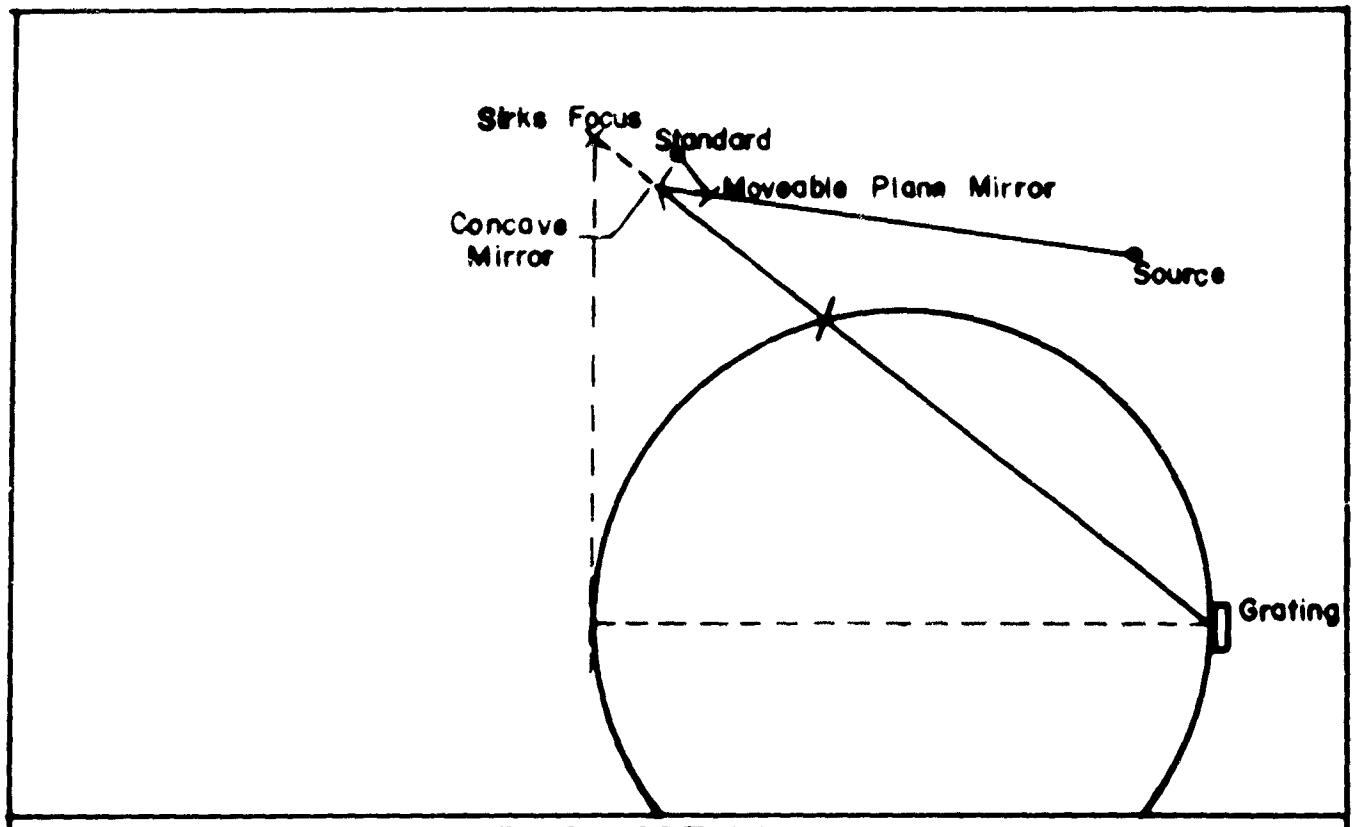

FIG 3a GRATING OPTICS

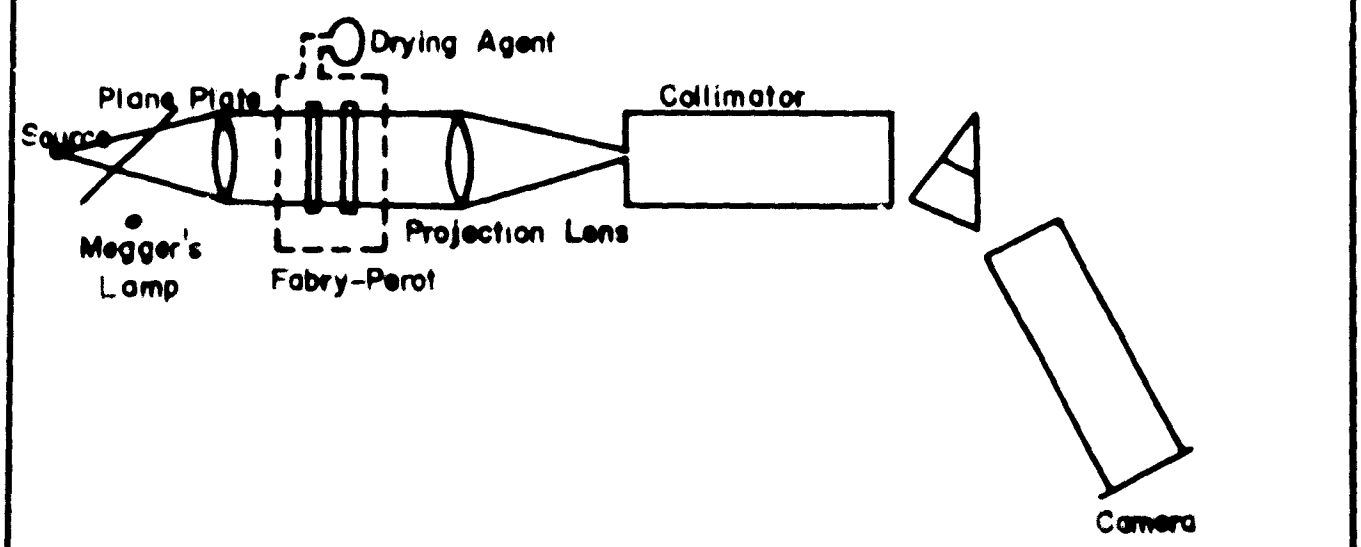

FIG 3b INTERFEROMETER OPTICS

Fig 4 Dispersion of Phase Change Curve

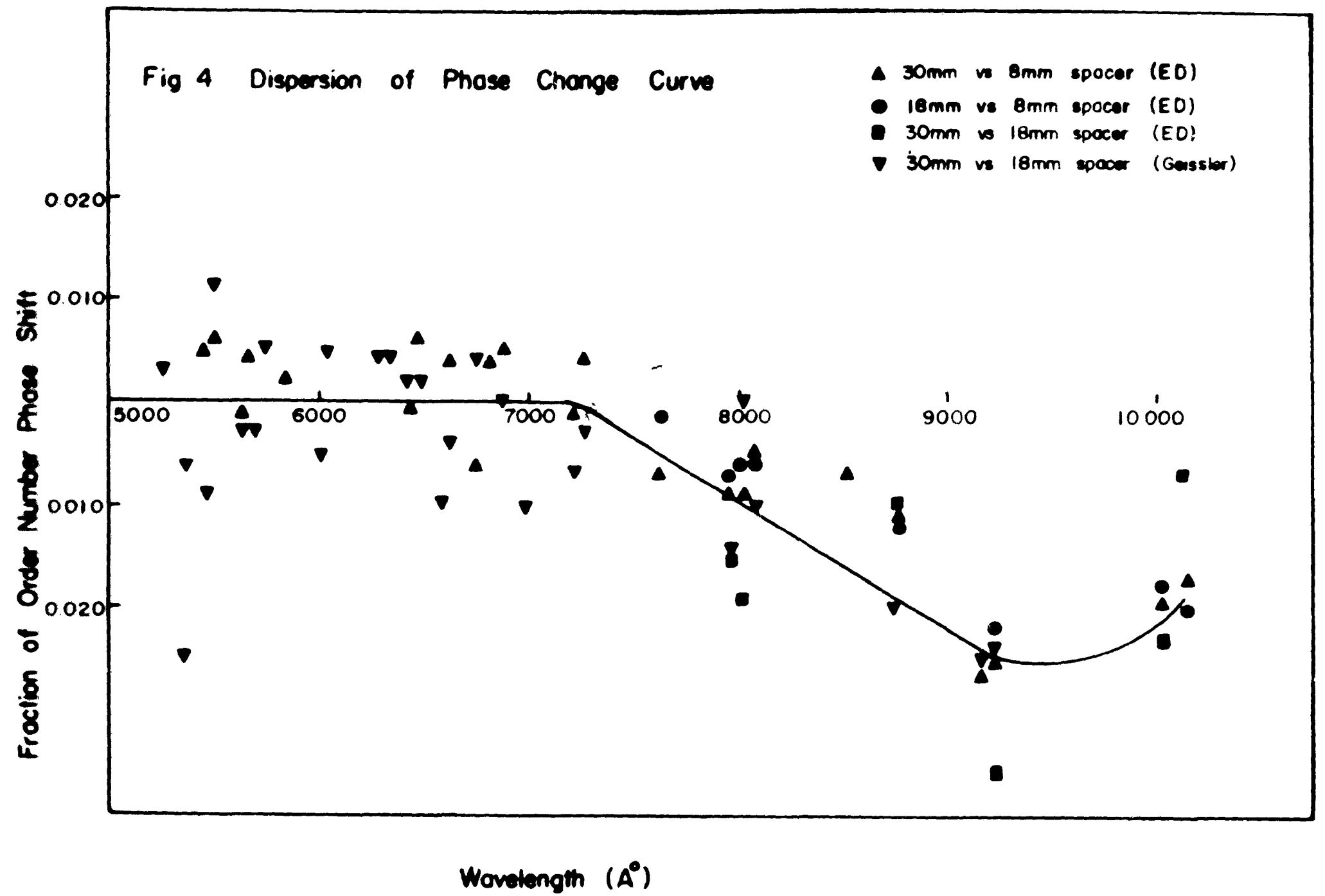

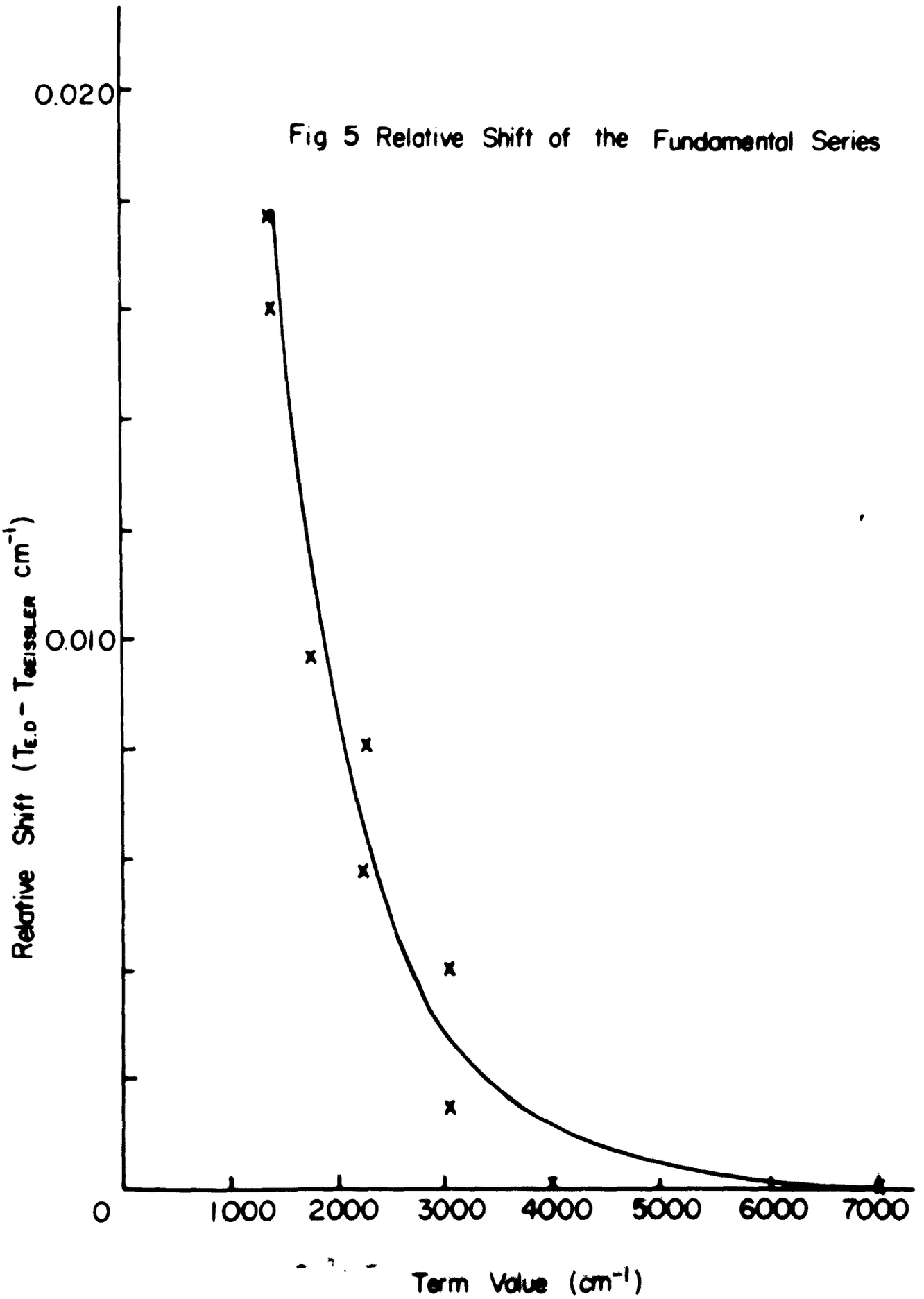

Fig 5 Relative Shift of the Fundamental Series

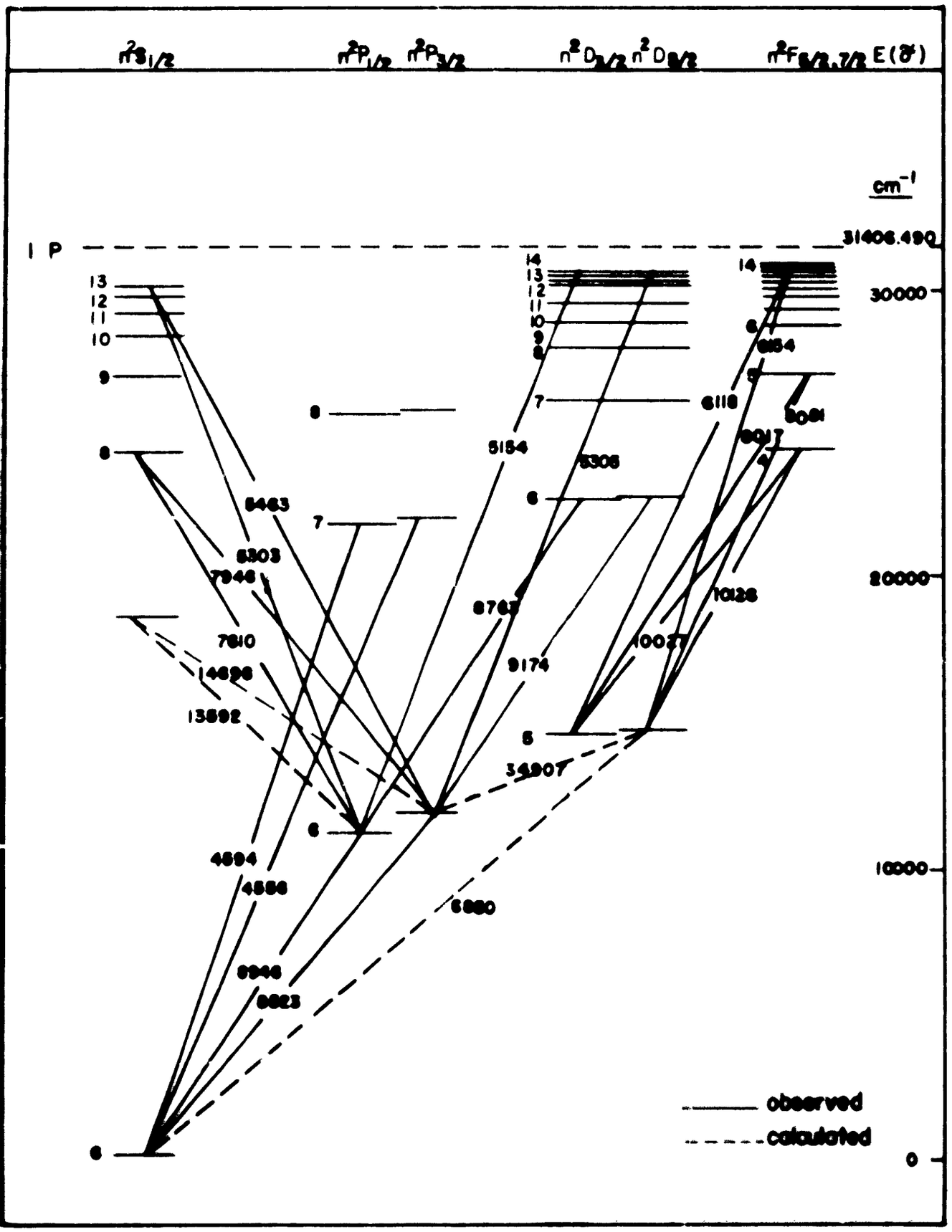

FIG 6 LEVEL SCHEME OF CESIUM I

Fig 8 Series Limit

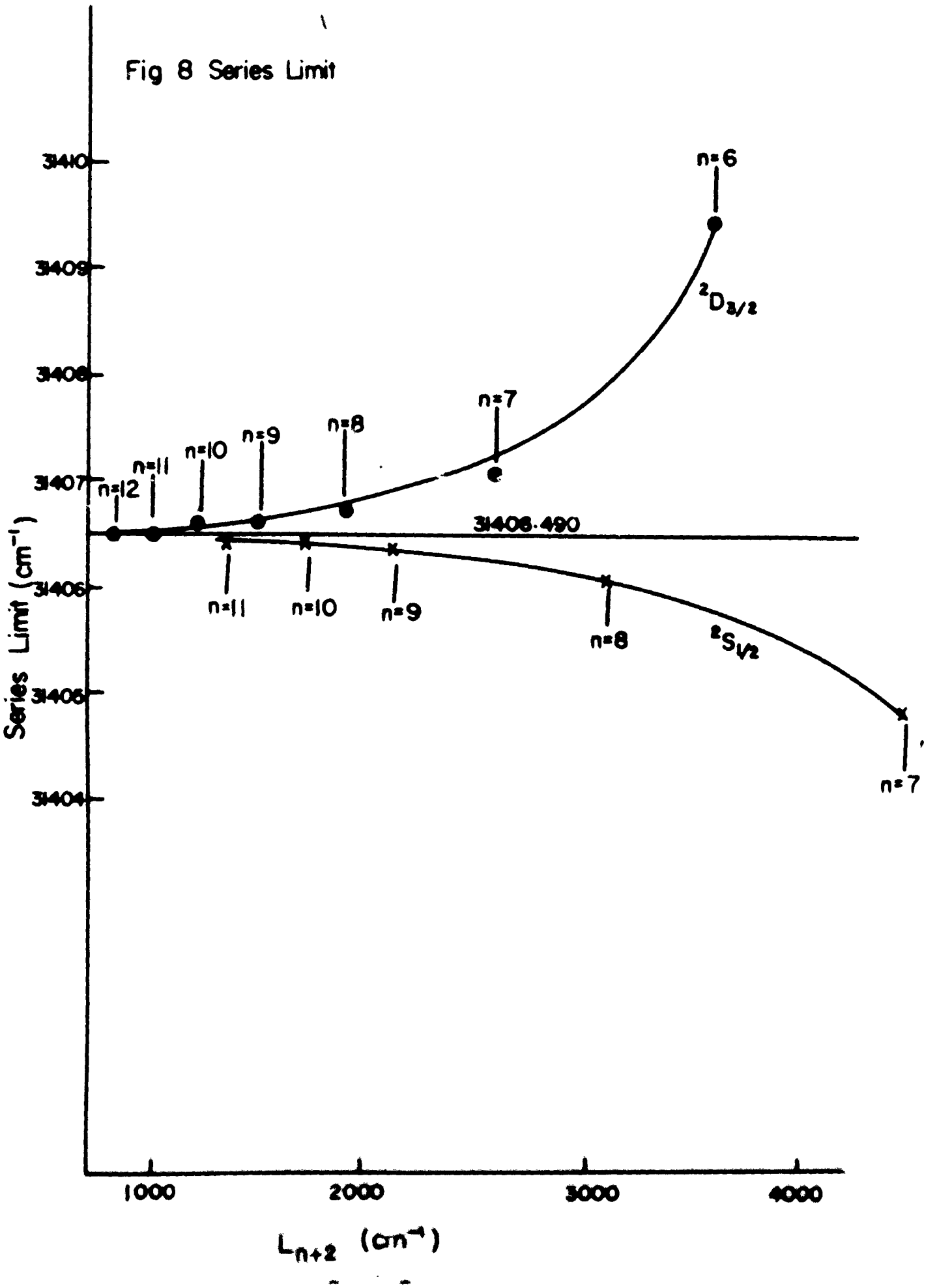

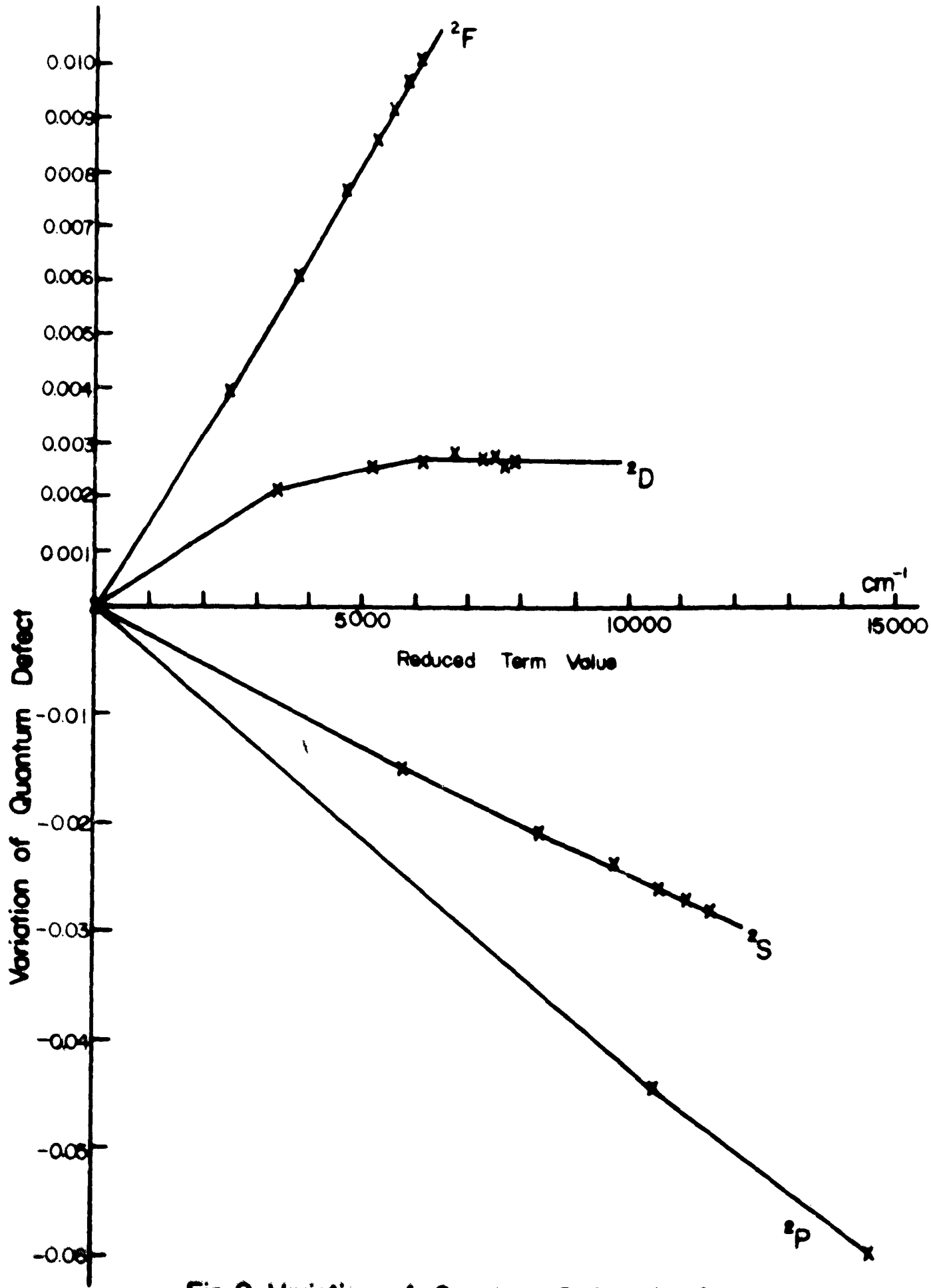

Fig 9 Variation of Quantum Defect in Cesium